Solar Dynamo and Toroidal Field Instabilities*

Alfio Bonanno

Abstract The possibility of non-axisimmetric (kink) instabilities of a toroidal field seated in the tachocline is much discussed in the literature. In this work, the basic properties of kink and quasi-interchange instabilities, produced by mixed toroidal and poloidal configuration, will be briefly reviewed. In particular it will be shown that the unstable modes are strongly localized near the Equator and not near the Poles as often claimed in the literature. Based on the results of recent numerical simulations, it is argued that a non-zero helicity can already be produced at a non-linear level. A mean-field solar dynamo is then constructed with a *positive* α-effect in the overshoot layer localized near the Equator and a meridional circulation with a deep return flow. Finally, the possibility that the solar cycle is driven by a $\alpha\Omega$ dynamo generated by the negative subsurface shear in the supergranulation layer will also be discussed.

Keywords: Solar dynamo; Magnetic fields

1. Introduction

An essential ingredient of any dynamo model is the α-effect, where α is the transport coefficient of the closure relation for the turbulent electromagnetic force. Owing to its pseudoscalar nature this term represents a likely possibility to produce a dynamo action with an axially symmetric field.

From the theoretical point of view it is expected that both the kinetic helicity $\langle \mathbf{v} \cdot \boldsymbol{\nabla} \times \mathbf{v} \rangle$ and the current helicity $\langle \mathbf{b} \cdot \boldsymbol{\nabla} \times \mathbf{b} \rangle$ produced by the velocity $\mathbf{v}$ and magnetic field $\mathbf{b}$ fluctuations contribute to this term (Gruzinov and Diamond, 1994), although the relative importance of these terms is still a subject of debate (Silant'ev, 2000). On physical grounds it is conceivable that in the bulk of the convection zone "cyclonic" turbulence (Parker, 1955) could be an efficient mechanism to produce a turbulent dynamo whose α-effect is dominated by the kinetic helicity (Steenbeck *et al.*, 1966).

The discovery, due to the interpretation of helioseismic data (Schou, 1991), that the stable stratified region below the convection zone is characterized by the presence of a strong horizontal shear (Kosovichev, 1996) has suggested the

possibility of an α-effect located just beneath the convection zone (Parker, 1993) in the region called the tachocline (Spiegel and Zahn, 1992). This fact has opened the door to the possibility that the source of the α-effect can have a magnetic origin, which can thus be attributed to various possible MHD instabilities (Ferriz-Mas *et al.*, 1994; Dikpati and Gilman, 2001; Chatterjee *et al.*, 2004). More recently, Bonanno and Urpin (2011, 2012) have further clarified a few aspects of kink and quasi-interchange instabilities in stably stratified plasma. While kink instabilities are generated from a pure toroidal field, quasi-interchange instabilities are produced by a mixed combination of the poloidal and toroidal field and their spectrum can be rather different from simple kink waves. It has also been shown that kink modes in spherical geometry are more effective near the Equator, a result that support the possibility of producing a non-zero α-effect at low latitudes. In fact, although the presence of a poloidal field breaks the symmetry creates a preferred helicity in the turbulence flow, Del Sordo *et al.* (2012) recently argued that kink instabilities alone can produce a preferred chirality in the turbulent plasma due to a symmetry-breaking effect at non-linear level.

In this article, after reviewing the basic properties of kink and quasi-kink instabilities in a stably stratified plasma, the possibility of explicitly constructing a solar dynamo with an α-effect localized at the bottom of the convective zone and at low latitudes will be discussed and compared to mean-field models where the α-effect is instead localized near the surface layer, as proposed by Brandenburg (2005).

2. Quasi-Interchange Instabilities in a Stably Stratified Plasma

The stability of a stably stratified column of plasma in the ideal MHD limit is the central problem of most of the controlled-fusion literature. In this context, the energy principle (Bernstein, 1958) has extensively been used in the past to study the stability of poloidal or toroidal fields (Tayler, 1973a,b) and also of mixed combinations of both (Tayler, 1980).

In cylindrical geometry, it can be proven that the plasma is stable for all azimuthal and vertical wave numbers (m and k), if it is stable for $m = 0$ in the $k \to 0$ limit, and for $m = 1$ for all k (Goedbloed *et al.*, 2004). On the other hand, to show that a generic configuration with a combination of axial field and non-homogenous azimuthal field is stable against the $m = 1$ mode (for all k) is not an easy task in general and one has to resort either to a variational approach or to a numerical investigation of the full eigenvalue problem in the complex plane. In this respect, the "normal mode" approach can be more useful in astrophysics, as it is often important to know the growth rate of the instability and the properties of the spectrum of the unstable modes (Bonanno and Urpin, 2008a,b). In particular, generic combinations of axial and azimuthal fields are subject to a class of resonant MHD waves that can never be stabilized for any value of the ratio of poloidal and toroidal fields. The instability of these waves has a mixed character, being both current- and pressure-driven. In this case the most rapidly growing unstable modes are resonant, *i.e.* the wave vector

$\mathbf{k} = (m/s)\mathbf{e}_\theta + k_z\mathbf{e}_z$ is perpendicular to the magnetic field, $\mathbf{B} \cdot \mathbf{k} = 0$ where k_z is the wavevector in the axial direction, m is the azimuthal wavenumber, and s is the cylindrical radius. The length scale of this instability depends on the ratio of poloidal and azimuthal field components and it can be very short, while the width of the resonance turns out to be extremely narrow. For this reason its excitation in simulations can be problematic.

It is interesting to have a qualitative understanding of the MHD spectrum for a simple cylindrical plasma equilibrium configuration consisting of a mixed configuration of an azimuthal B_ϕ and a constant axial field B_z. As was shown in Bonanno and Urpin (2011), for a generic disturbance of the form $e^{(\sigma t - ik_z z - im\varphi)}$ an approximate expression for the dimensionless growth rate $[\Gamma = \sigma/\omega_{A\phi}]$ being $\omega_{A\phi}$ the Alfvén frequency in the azimuthal direction, is given by

$$\Gamma^2 = \frac{2m^2(\alpha - 1)}{m^2 + (p^2 + m^2)\varepsilon^2}, \tag{1}$$

where p is the dimensionless radial wavenumber, $\varepsilon = B_z/B_\varphi$, $\alpha = \partial \ln B_\varphi / \partial \ln s$, and s is the cylindrical radius. Moreover the dimensionless vertical wavenumber $[q = k_z s]$ is close to the resonance condition $[f \equiv q\varepsilon + m \approx 0]$ which implies that the total Alfvén frequency is zero $[\omega_A = \mathbf{B} \cdot \mathbf{k}/\sqrt{4\pi\rho} = 0]$ at the resonance. The instability is never suppressed for any finite value of ε and the growth rate is a rapidly increasing function of m in particular $\Gamma^2 \approx (1 + \varepsilon^2)^{-1}$ in the limit $m \gg p^2$. If $\alpha < 1$, it is possible to show that

$$\Gamma^2 \approx f^2 \frac{1 + \alpha}{1 - \alpha}, \tag{2}$$

that implies instability if $\alpha > -1$. The profile with $\alpha < -1$ is stable in this approximation. Note that modes with q satisfying the resonance condition $\omega_A = 0$ (or $f = 0$) are marginally stable because $\Gamma = 0$ for them, but $\Gamma^2 > 0$ in a neighborhood of the resonance. Therefore, the dependence of Γ on q should have a two-peak structure for any m. As in the case $\alpha > 1$, the instability occurs for any value of ε. If $\alpha = 1$, then we have

$$\Gamma^2 \approx \mu f \left[\frac{2m}{m^2 + q^2} \pm \sqrt{\frac{4m^2}{(m^2 + q^2)^2} + 4\mu} \right]. \tag{3}$$

where μ is a positive number of the order unity. In this case, the dependence $\Gamma^2(q)$ also has a two-peak structure because $\Gamma = 0$ at the resonance but $\Gamma^2 > 0$ in its neighborhood. The instability is always present for any finite value of ε. This explicit solution shows that, if $\alpha > -1$, the instability always occurs for disturbances with q and m close to the condition of magnetic resonance, $\omega_A = 0$. The axial field cannot suppress the instability which occurs even if B_z is significantly greater than B_φ.

3. Kink Instabilities below the Tachocline

Can the instabilities described in the previous section be operative in the overshoot layer of the Sun, or even below? To address this question we must consider

the problem in spherical geometry, including the stabilizing effect of gravity and the destabilizing effect of thermal diffusivity. In fact the stability of the spherical magnetic configurations has been studied in much less detail and even the overall stability properties of stellar radiation zones are rather unclear. **?** studied the stability of a random initial field in the stellar radiative zone by direct numerical simulations, and it was found that the stable magnetic configurations generally have the form of tori with comparable poloidal and toroidal field strengths. The possible relaxation mechanism was further discussed by Duez and Mathis (2010). The stability of azimuthal fields near the rotation axis has also been studied by Spruit (1999). The author used a heuristic approach to estimate the growth rate and criteria of instability. Unfortunately, many of these estimates and criteria are misleading because they do not apply in the main fraction of the volume of a radiation zone where the stability properties can be qualitatively different. The heuristic approach was criticized by Zahn *et al.* (2007). The stability of the toroidal field in rotating stars has been considered by Kitchatinov (2008) and Kitchatinov and Rüdiger (2008) who argued that the magnetic instability is essentially three-dimensional and determined the threshold field strength at which the instability sets. Estimating this threshold in the solar radiation zone, the authors impose an upper limit on the magnetic field ≈ 600 G.

The problem has recently been investigated by Bonanno and Urpin (2012) where it was shown that the most unstable modes have low radial wavelengths at variance with the claim of Kitchatinov and Rüdiger (2008). Moreover if the thermal conductivity is considered, no threshold field is needed to trigger the instability. The most interesting result is illustrated by the angular dependence of the growth rate, as can be seen in Figure 1 where it appears that the instability is effective mostly near the Equator, and not along the axis, as originally supposed by Tayler (1973a). In general the location of the most unstable latitude depends also on the geometry of the basic state and cannot be determined only by local instability criteria.

Can this instability produce an α-effect? It is difficult to consistently compute the strength of the α-effect within the linear analysis alone, although a first estimation in this direction has been provided by Rüdiger *et al.* (2011). However, recent investigations in cylindrical symmetry pointed out that it is possible to generate a non-zero helicity out of a kink instability due to non-linear effects (Del Sordo *et al.*, 2012; Bonanno *et al.*, 2012).

4. Flux-Transport Dynamo and Tachocline α-Effect

The previous discussion put forward that a likely location of the α-effect generated by current-driven instabilities is precisely in the overshoot layer with a strong concentration of the turbulence at low latitudes where the instability is more effective. Although only 3D numerical simulations can in principle determine the full structure of the α-tensor, as a first step in building a realistic model we can consider a latitudinal dependence of the type $\cos\theta\sin^2\theta$ to model the suppression of the α-effect near the poles. The other essential ingredient is the inclusion of the meridional circulation. In fact, in the presence of a low eddy

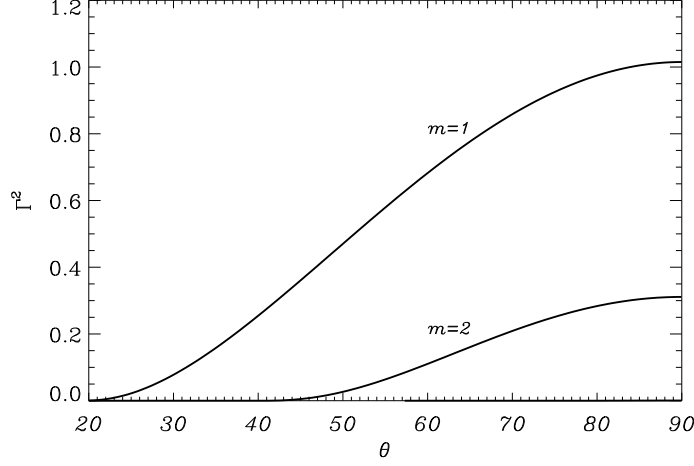**Figure 1.** The dimensionless growth rate of the fundamental radial mode as a function of the polar angle, θ, for $\ell = 5$, $m = 1, 2$, and $d = 0.1$ in the case of a neutral stratification. Note that ℓ is the latitudinal "quantum" number of the perturbation. See Bonanno and Urpin (2012) for further details.

diffusivity [η_t] (as is likely to be in the overshoot region), the magnetic Reynolds number becomes very large and the dynamics of the mean-field flow becomes an essential ingredient of the dynamo process. In this regime the advection produced by the meridional circulation dominates the diffusion of the magnetic field which is then transported by the meridional circulation (Dikpati and Charbonneau, 1999; Dikpati and Gilman, 2001; Küker *et al.*, 2001; Bonanno *et al.*, 2002; Chatterjee *et al.*, 2004; Bonanno *et al.*, 2006; Guerrero and de Gouveia Dal Pino, 2008).

The magnetic induction equation reads

$$\frac{\partial \mathbf{B}}{\partial t} = \boldsymbol{\nabla} \times (\mathbf{U} \times \mathbf{B} + \alpha \mathbf{B}) - \boldsymbol{\nabla} \times (\eta_{\mathrm{T}} \boldsymbol{\nabla} \times \mathbf{B}), \tag{4}$$

where η_{T} is the turbulent diffusivity. Axisymmetry implies that relative to spherical coordinates the magnetic field ($\mathbf{B}$) and the mean flow field ($\mathbf{U}$), respectively, read

$$\mathbf{B} = B(r, \theta, t)\mathbf{e}_\phi + \boldsymbol{\nabla} \times [A(r, \theta, t)\mathbf{e}_\phi]$$

$$\mathbf{U} = \mathbf{u}(r, \theta) + r \sin \theta \Omega(r, \theta)\mathbf{e}_\phi$$

being $A(r, \theta, t)$ the vector potential. The meridional circulation [$\mathbf{u}(r, \theta)$] and differential rotation [$\Omega(r, \theta)$] are the poloidal and toroidal components of the global velocity flow field [$\mathbf{U}$]. In particular the poloidal and toroidal components

of Equation (4) respectively determine

$$\frac{\partial A}{\partial t} + \frac{1}{s}(\mathbf{u}\cdot\boldsymbol{\nabla})(sA) = \alpha B + \frac{\eta_{\mathrm{T}}}{r}\frac{\partial^2(rA)}{\partial r^2} + \frac{\eta_{\mathrm{T}}}{r^2}\frac{\partial}{\partial\theta}\Big(\frac{1}{s}\frac{\partial(sA)}{\partial\theta}\Big),\tag{5a}$$

$$\frac{\partial B}{\partial t} + s\rho(\mathbf{u}\cdot\boldsymbol{\nabla})\Big(\frac{B}{s\rho}\Big) = \frac{\partial\Omega}{\partial r}\frac{\partial(A\sin\theta)}{\partial\theta} - \frac{1}{r}\frac{\partial\Omega}{\partial\theta}\frac{\partial(sA)}{\partial r} + \frac{1}{r}\frac{\partial}{\partial r}\Big(\eta_{\mathrm{T}}\frac{\partial(rB)}{\partial r}\Big)$$
$$+\frac{\eta_{\mathrm{T}}}{r^2}\frac{\partial}{\partial\theta}\Big(\frac{1}{s}\frac{\partial(sB)}{\partial\theta}\Big) - \frac{1}{r}\frac{\partial}{\partial r}\Big(\alpha\frac{\partial(rA)}{\partial r}\Big) - \frac{\partial}{\partial\theta}\Big(\frac{\alpha}{\sin\theta}\frac{\partial(A\sin\theta)}{\partial\theta}\Big),\tag{5b}$$

where $s = r\sin\theta$. The α-effect and the turbulent diffusivity are parametrized by means of

$$\alpha = \frac{1}{4}\,\alpha_0\cos\theta\sin^2\theta\Big[1 + \mathrm{erf}\Big(\frac{x - a_1}{d}\Big)\Big]\Big[1 - \mathrm{erf}\Big(\frac{x - a_2}{d}\Big)\Big],$$
$$\eta = \eta_c + \frac{1}{2}(\eta_t - \eta_c)\Big[1 + \mathrm{erf}\Big(\frac{r - r_\eta}{d_\eta}\Big)\Big],\tag{6}$$

where α_0 is the amplitude of the α-effect, $x = r/R_\odot$ is the fractional radius, a_1, a_2 and d define the location and the thickness of the turbulent layer, η_t is the eddy diffusivity, η_c the magnetic diffusivity beneath the convection zone and d_η represents the width of this transition. In this investigation, the values $a_1 = 0.67$, $a_2 = 0.72$, and $d_\eta = 0.025$ have been used.

The components of the meridional circulation can be represented with the help of a stream function $\Psi(r,\theta) = -\sin^2\theta\cos\theta\,\psi(r)$ so that

$$u_r = \frac{1}{r^2\rho\sin\theta}\frac{\partial\Psi}{\partial\theta}, \quad u_\theta = -\frac{1}{r\rho\sin\theta}\frac{\partial\Psi}{\partial r}\tag{7}$$

with the consequence that the condition $\boldsymbol{\nabla}\cdot(\rho\mathbf{u}) = 0$ is automatically fulfilled. A strategy to constrain several properties of the meridional circulation is to assume the differential rotation profile $\Omega(r,\theta)$ as a given ingredient, and deduce an approximation for the function ψ from the angular-momentum conservation along the azimuthal direction. An approximate expression for ψ is thus

$$\psi \approx \frac{5\rho r}{2\Omega_{\mathrm{eq}}}\int_0^\pi \langle u_r u_\theta\rangle\mathrm{d}\theta\tag{8}$$

where Ω_{eq} is the equatorial angular velocity. In particular, for the standard, isotropic mixing-length theory, Equation (8) becomes (Durney, 2000)

$$\psi \approx -\frac{5\rho r}{2\Omega_{\mathrm{eq}}}\langle u_r^2\rangle\,.\tag{9}$$

In principle it would be possibile to explicitly compute ψ and ψ' using the relation (9) knowing the convective velocities of the underlying stellar model. In practice this would be problematic, because the convective fluxes and their radial derivatives computed from standard mixing-length theory are discontinuous at the base of the convective zone. In a more realistic situation the presence of an overshoot layer implies that $\langle u_r^2\rangle \to 0$ smoothly so that u_θ is continuous at the

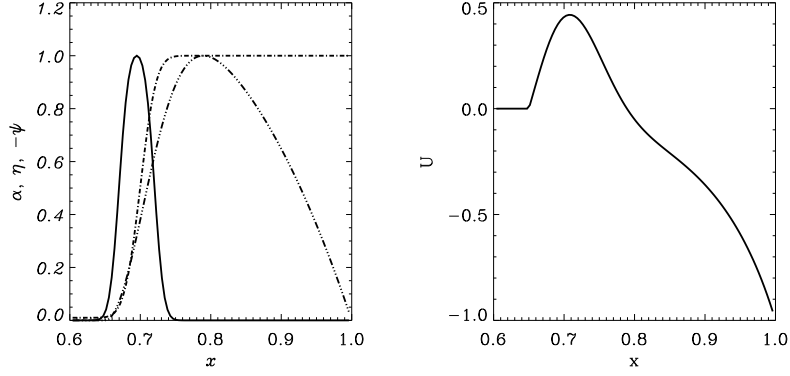**Figure 2.** The α-effect (solid line), turbulent diffusivity (dot-dashed line) and (minus) the function $\psi(r)$ (dot-dot-dot dashed line), are depicted in the left panel. The meridional circulation in units of the maximum surface value at a latitude of $45°$ is instead depicted in the right panel.

inner boundary. Nevertheless one can use the representation (9) to determine the stagnation point where $\psi' = 0$, which turns out to be around $x = 0.8$ in terms of the fractional radius. An explicit form of the function ψ which incorporates the following features reads

$$\psi = C \left[1 - \exp\left(-\frac{(x - x_b)^2}{\sigma^2} \right) \right] (x - 1)\, x^2 , \qquad (10)$$

where C is a normalization factor, $x_b = 0.65$ defines the penetration of the flow, $\sigma = 0.08$ measures how rapidly $\langle u_r^2 \rangle$ decays to zero in the overshoot layer and the location of the stagnation point. The density profile is taken to be $\rho = \rho_0 \left(\frac{1}{x} - x_0 \right)^m$ in which m is an index representing the the stratification of the underlying solar model, its value in the region of interest is approximately 1.5, and $x_0 = 0.85$, so that with these value the strength of the meridional circulation at low latitudes is of the same order as the surface flow, as discussed by Bonanno (2012); see also Pipin and Kosovichev (2011) for a similar investigation. The radial profile of the α-effect, turbulent diffusivity, stream function and meridional circulation used in the calculation are depicted in Figure 2.

The helioseismic profile for the differential rotation is taken so that

$$\Omega(r, \theta) = \Omega_c + \delta\left(\frac{r - r_c}{d_c} \right) (\Omega_s(\theta) - \Omega_c), \qquad (11)$$

where $\Omega_c/2\pi = 432.8$ nHz is the uniform angular velocity of the radiative core, $\Omega_s(\theta) = \Omega_{eq} + a_2 \cos^2\theta + a_4 \cos^4\theta$ is the latitudinal differential rotation at the surface and $\delta(x) \equiv (1 + \text{erf}(x))/2$. In particular $\Omega_{eq}/2\pi = 460.7$ nHz is the angular velocity at the Equator, $a_2/2\pi = -62.9$ nHz, and $a_4/2\pi = -67.13$ nHz. In this calculation the angular velocity is normalized in terms of equatorial differential rotation Ω_{eq}, $r_c = 0.71$ and $d_c = 0.025$. As usual, the dynamo equations can
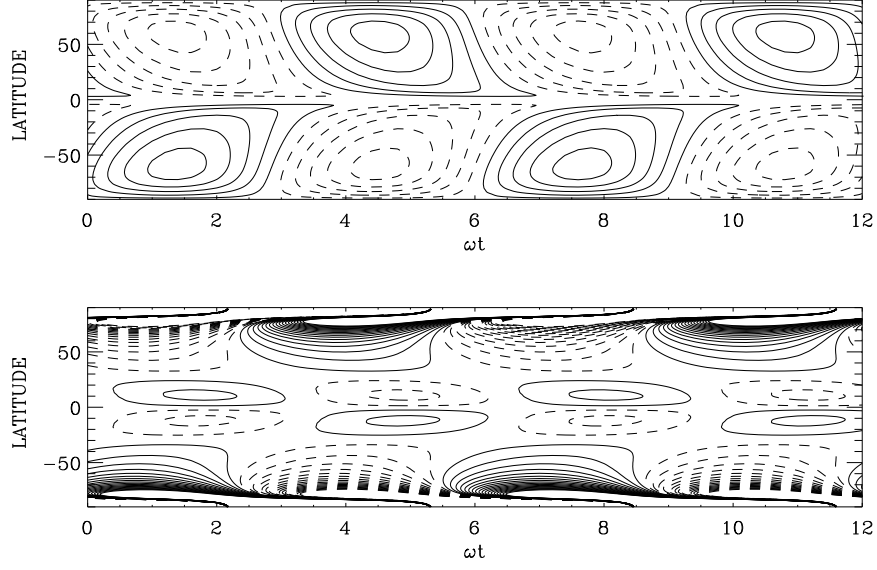
Figure 3. Butterfly diagram for a solution with meridional circulation included. The isocontours for the toroidal field (upper panel) at the base of the convection zone and the radial field on the top boundary are shown. Full and dashed lines show the positive and negative levels respectively. The solution is obtained with $C_\alpha = 2$, $C_\Omega = 4.5 \times 10^5$ and $C_u = 400$ which implies a period of about 24 years a turbulent diffusivity $\eta_t = 3.1 \times 10^{11}$ cm^2 s^{-1} and a (poleward) surface flow of about 18 m s^{-1}. It is interesting to notice that at low latitude the phase relation is consistent with the observations, namely $B_r B_\phi < 0$. This type of solution also shows a strong preference for dipolar modes. In particular the critical solution for the symmetric mode has $C_\alpha = 3.70$, significantly greater than the antisymmetric mode. An essential ingredient in order to get this property correct is the presence of a strong meridional circulation at the bottom of the convective zone. In particular in this case the bottom flow is about 8.5 m s^{-1}.

be made dimensionless by introducing the dynamo numbers $C_\Omega = R_\odot^2 \, \Omega_{\text{eq}}/\eta_T$, $C_\alpha = R_\odot \alpha_0/\eta_T$, $C_\omega = R_\odot \omega/\eta_T$, $C_u = R_\odot U/\eta_T$, where ω is the frequency of the dynamo wave, and $U = u_\theta(r = R_\odot, \theta = 45°)$. This linear dynamo problem is solved with a finite-difference scheme for the radial dependence and a polynomial expansion for the angular dependence by imposing potential field as a boundary condition for the surface, and perfect conductor for the inner boundary. Further details of the numerical approach can be found in Bonanno *et al.* (2002, 2006) and also in Jouve *et al.* (2008).

A reference solution can be then obtained in the region of high C_u, and its main properties are the following: $C_\alpha = 2$, $C_\Omega = 4.5 \times 10^5$, and $C_u = 400$ which implies a period of about 24 years, a turbulent diffusivity $\eta_t = 3.1 \times 10^{11}$ cm^2 s^{-1} and a (poleward) surface flow of about 18 m s^{-1}. The basic properties of this solution are depicted in Figure 3 where the butterfly diagram for the toroidal field at the bottom of the convection zone, and of the radial field at the surface are shown. It is interesting to notice that at low latitude the phase relation is consistent with the observations, namely $B_r B_\phi < 0$. The other property of this

solution is that it shows a strong preference for dipolar modes. In particular the critical solution for the symmetric mode has $C_\alpha = 3.70$, significantly greater than the antisymmetric mode. On the contrary, had we considered the case of an α-effect uniformly distributed throughout the whole of the convection zone, the result would have been $C_\alpha = 2.1$ for both symmetric and antisymmetric mode with a difference of about 1% most probably due to numerics. The conclusion is that the parity of the solution is more likely to be a dipole if the α-effect is located at the bottom of the convection zone. In our simulations the precise value of the ratio η_c/η_t was not crucial as we obtained basically the dynamo solution for $\eta_c/\eta_t = 0.005$ and $\eta_c/\eta_t = 0.05$ although in all of the simulations presented in this work the value $\eta_c/\eta_t = 0.01$ has been chosen. For instance the period obtained for $\eta_c/\eta_t = 0.005$ was 24.9 years, and for $\eta_c/\eta_t = 0.05$ was 24.5 years. This is not surprising as the penetration of the meridional flow is very weak as showed in the right panel of Figure (2) and therefore the precise value of η_c cannot significantly change the type of dynamo action. In addition, changing the width of the α effect and of the turbulent diffusivity also did not lead to significant changes in the solution, although we expect that the spatial extension of the turbulent layer should be of the order of the tachocline width $d_\eta \approx 0.05$ solar radii.

However, the serious, unsatisfactory aspect of advection dominated dynamo is the fact that the strength of the return flow is largely unknown, and the eddy diffusivity is about one order of magnitude greater than would be expected on the basis of the standard mixing length theory.

5. Solar Dynamo from Subsurface Shear Instabilities

In recent years the possibility that the dynamo operates in the subphotospheric layers of the Sun mostly driven by the negative gradient of the angular velocity near the surface has been proposed (Brandenburg, 2005). It is interesting to see if a mean-field dynamo model can describe this case with the help of a more refined differential-rotation profile including the negative shear in the subsurface layers. In order to discuss this issue a slightly modified version of the analytical approximation presented in Dikpati *et al.* (2002) has been used. The radial profile of the α-effect and turbulent diffusivity are depicted in Figure (4). In particular the rotation rate is taken constant in the radiative interior $[\Omega_c]$ and the tachocline is located at the same radius as in the model described in the previous session. It is assumed that has constant width $\approx 0.05 R_\odot$, and at the top of the tachocline its rotation rate is given by

$$\Omega(r_{\mathrm{cz}}, \theta) = \Omega_{\mathrm{cz}} + a_2 \cos^2 \theta + a_4 \cos^4 \theta \tag{12}$$

where $\Omega_{\mathrm{cz}} = -a_2/5 - 3\, a_4/35$, $a_2 = -61$ nHz and $a_4 = -73.5$ nHz. It is thus assumed that there is a known negative gradient below the surface down to a radius $r_s = 0.95 R_\odot$ and the latitudinal dependence of this shear layer is modeled by $P(\theta) = (p_0 + p_4 \cos^4 \theta)/R_\odot$, so that

$$\Omega(r, \theta) = \Omega_c + \delta\left(\frac{r - r_c}{d_c}\right) Q(\theta)(r - r_{cz}) + \delta\left(\frac{r - r_s}{d_s}\right)[\Omega(r_{\mathrm{cz}}, \theta) - \Omega_c]$$
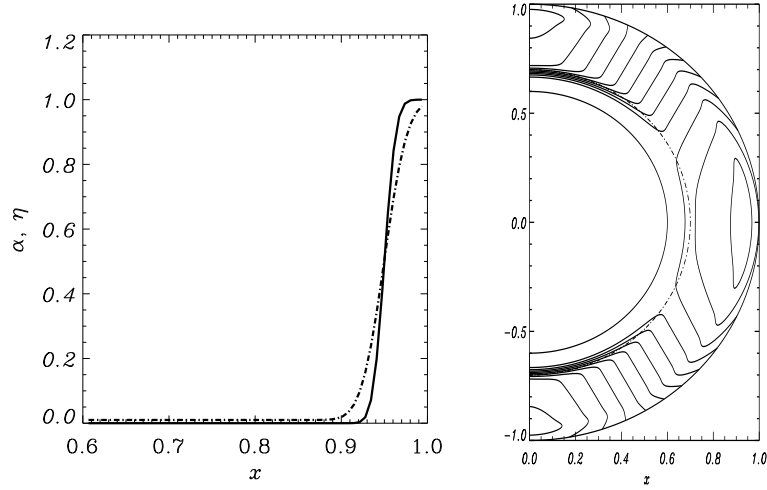
Figure 4. Left panel: the α-effect profile (solid line) and turbulent diffusivity (dot-dashed line) used for an $\alpha\Omega$ model with a dynamo action produced from subsurface shear instabilities. Right panel: the isocontour lines of the differential rotation $[\Omega(r,\theta)]$ in units of the equatorial rotation. Note the negative shear near the surface around $r/R_\odot \approx 0.95$.

$$+\delta\left(\frac{r-r_s}{d_s}\right)[\Omega_{eq}-\Omega_{cz}-P(\theta)(r-R_\odot)-Q(\theta)(r-r_{cz})] \tag{13}$$

and $Q(\theta)=(\Omega_{eq}-\Omega_{cz}+P(\theta)(R_\odot-r_s))/(r-r_{cz})$. For actual calculations the values $p_0=437$ nHz and $p_4=-722$ nHz have been chosen. In order to confine the magnetic field in the subsuface layers it is assumed that η_t is also maximum near the surface, and it sharply decreases by about two orders of magnitude just below the supergranulation layer where the α-effect is located. The basic features of the (critical) dynamo solution in this case is depicted in Figure 5 for a solution with $C_\alpha=18$, $C_\Omega=1\times10^3$ which implies a period of about four years and a turbulent diffusivity $\eta_t=1.4\times10^{13}$ cm^{2}s^{-1}. The period is clearly too small, but this is not surprising as the dynamo wave is basically entirely confined in the surface layers as can be seen in Figure (6). The only possibility to match the solar period is to further increase the turbulent diffusivity in the supergranulation layer, but this would imply that the spatial extension of the dynamo wave propagates deeply within the convective zone, thus preventing the negative radial shear to produce the correct butterfly diagram. Moreover the parity of the solution is clearly symmetric because $C_\alpha=15$ for quadrupolar modes.

6. Conclusions

Where is the α-effect located in the Sun? Despite the difficulties present in models of flux-dominated dynamo (too low eddy diffusivity, unknown strength and location of the return flow), mean-field models with an α-effect located at
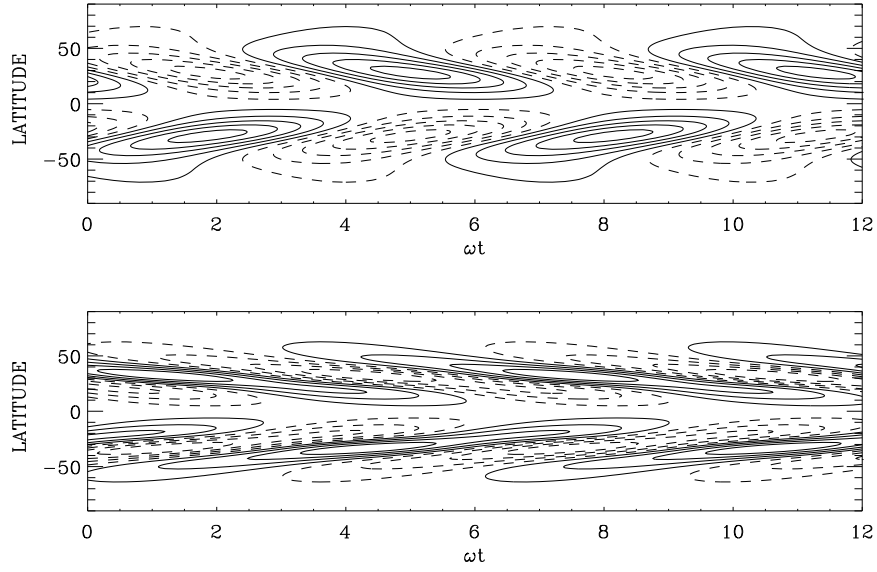
Figure 5. Butterfly diagram for a model with strong radial subsurface shear. The isocontours for the toroidal field (upper panel) at $r = 0.95R$ and the radial field on the top boundary are shown. Full and dashed lines show the positive and negative levels respectively. The solution is obtained with $C_\alpha = 18$ and $C_\Omega = 1 \times 10^3$ which implies a period of about four years and a turbulent diffusivity $\eta_t = 1.4 \times 10^{13}$ cm^{2}s^{-1}.

the bottom of the convective zone are successful in reproducing several aspects of the solar activity cycle. In this model the origin of the α-effect is due to the turbulent magnetic helicity and current helicity generated by the quasi-interchange instabilities below the tachocline and does not follow from mixing-length theory. The most striking result comes from the parity of the solution: only with an α-effect located at the bottom of the convective zone the dipolar modes are most easily excited, at least at the linear level. This result also apply for models with the α-effect generated by the subsurface shear, the solutions are mostly symmetric, rather than anti-symmetric. It would be nice to see if a more realistic surface boundary condition can solve this problem as proposed by Pipin and Kosovichev (2011).

Although the models discussed in the previous session are kinematic, it is difficult to believe that the discussion of the previous session will drastically change if a non-linearity via the α-quenching is included in the models. Jouve *et al.* (2008) present a code comparison between kinematic models and non-linear models that shows that the critical solutions are basically the same within the tolerance of different numerical schemes. On the other hand the advantage of the kinematic approach is to provide a complete view of the spectrum of the dynamo waves that can be excited for a given set of dynamo numbers. This is clearly an important piece of information for the non-linear simulations, for instance for investigating degenerate configurations due to the degeneracy in the spectrum.
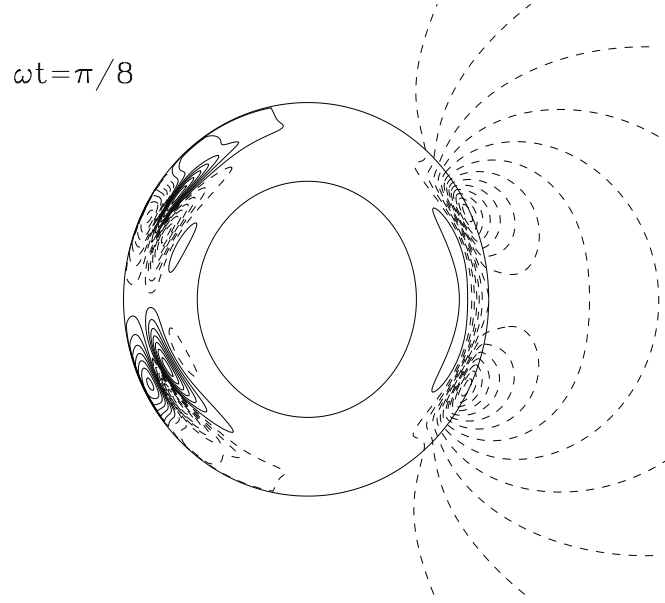
$$\omega t = \pi/8$$

Figure 6. Toroidal and poloidal field configuration for a typical dynamo solution with a strong subsurface shear, and $C_\alpha = 18$, $C_\Omega = 1 \times 10^3$. The left part are the isocontours line of the toroidal field, with solid line for negative B_ϕ and dashed line for positive value of the field. The right part represents the streamlines of the poloidal field given by contours of $Ar\sin\theta$. Solid line are for negative values of A. Note that the dynamo action is confined around the region of strongest radial shear, and, for this reason, the period tends to be rather short in general (less than ten years in these type of models).

An important constraint on the viability of a solar dynamo with a tachocline α-effect is the fact that successful models must have a *positive* α-effect: no migration is present for a negative α-effect. It would be an important check for the theory to show that this is actually the case by means of 3D global numerical simulations of the kink and quasi-interchange instability in spherical symmetry. Recent investigations in this direction in cylindrical symmetry have questioned this possibility (Gellert, Rüdiger and Hollerbach, 2001) although further numerical and analytical work is needed before a firm conclusion can be reached.

References

Bernstein, I.B., Frieman, E.A., Kruskal, M.D., Kulsrud, R.M. 1958, *Proc. Roy. Soc. Lond.*, **A244**, 17

Braithwaite, J. 2006, *Astron. Astrophys.* **453**, 687

Bonanno, A. arXiv:1112.4929B

Bonanno, A.; Elstner, D., Rüdiger, G., Belvedere, G. 2002, *Astron. Astrophys.* **390**, 673

Bonanno, A.; Elstner, D., Belvedere, G. 2006, Astron. Nachr., **327**, 680

Bonanno A., Urpin V. 2008, *Astron. Astrophys.* **477**, 35

Bonanno A., Urpin V. 2008, *Astron. Astrophys.* **488**, 1

Bonanno, A.; Urpin, V. 2011, Phys. Rev. E, **84**, 056310

Bonanno, A.; Urpin, V. 2012, *Astrophys. J.* **747**, 137

Bonanno, A.; Brandenburg, A., Del Sordo, F., Dhrubaditya, M., *Phys. Rev.* **E 86**, 016313, 2012 and arXiv:1204.0081.

Brandenburg, A. 2005, *Astrophys. J.* **625**, 539

Chatterjee, P.; Mitra, D., Rheinhardt, M., Brandenburg, A. 2011, *Astron. Astrophys.* **534**, 46

Chatterjee, P.; Nandy, D.; Choudhuri, A. R. 2004, *Astron. Astrophys.* **427**, 1019

Del Sordo, F., Bonanno, A., Brandenburg, A., Dhrubaditya, M., In: C.H. Mandrini (ed.) *Comparative Magnetic Minima: Characterizing quiet times in the Sun and star, IAU Symposium* **286**, Cambridge University Press, and arXiv:1111.1742.

Dikpati, M., Charbonneau, P. 1999, *Astrophys. J.* **518**, 508

Dikpati, M. and Gilman, P.A. 2001, *Astrophys. J.* **559**, 428

Dikpati, M., Corbad, T., Thompson, M.J., Gilman, P.A. 2002, *Astrophys. J.* 575, L41

Duez, V., Mathis. S. 2010, *Astrophys. J.* **517**, 58

Durney, B. R. 2000, *Astrophys. J.* **528**, 486

Gellert, M., Rüdiger G.,Hollerbach, R. 2011, *Mon. Not. Roy. Astron. Soc.* **414**, 2696

Ferriz-Mas, A. Schmitt, D., Schüssler, M. 1994, *Astron. Astrophys.* **289**, 949

Goedbloed, H., Poedts, S., *Principles of Magnetohydrodynamics*, Cambridge University Press, (2004)

Gruzinov, A.V.; Diamond, P.H. 1994, Phys. Rev. Lett., 72, 1651

Guerrero, G. and de Gouveia Dal Pino, E. M. 2008, *Astron. Astrophys.* 485, 267

Jouve *et al.* 2008, *Astron. Astrophys.* 483, 949960

Küker, M., Rüdiger, G., Schultz, M. 2001, *Astron. Astrophys.* **374**, 301

Kitchatinov, L. 2008, Astron. Rep. **52**, 247

Kitchatinov, L., Rüdiger, G. 2008, *Astron. Astrophys.* **478**, 1

Kosovichev, A.G. 1996, *Astrophys. J.* **269**, 61

Parker, E. N. 1955, *Astrophys. J.* **122**, 293

Parker, E. N. 1993, *Astrophys. J.* **408**, 707

Pipin, V.V., Kosovichev, A.G. 2011, *Astrophys. J.* **727**, L45

Pipin, V.V., Kosovichev, A.G. 2011, *Astrophys. J.* **738**, 104

Rüdiger, G., Kitchatinov, L., Elstner, D. 2012, *Mon. Not. Roy. Astron. Soc.* **425**, 2267 and arXiv:1107.2548.

Schou, J., 1991 In: *Challenges to Theories of the Structure of Moderate-Mass Stars*, Lecture Notes Phys. **388**, ed D.Gough & Toomre editors (Berlin), Springer, 81

Silant'ev, N.A. 2000, *Astron. Astrophys.* **364**, 449

Spiegel, E. A. and Zahn, J.-P. 1992, *Astron. Astrophys.* **265**, 106

Spruit, H. 1999, *Astron. Astrophys.* **349**, 189

Steenbeck, M., Krause, F., Rädler, K.H. 1966, *Z. Naturforsch.* **21a**, 369

Tayler R.J. 1973, *Mon. Not. Roy. Astron. Soc.* **161**, 365

Tayler R.J. 1973, *Mon. Not. Roy. Astron. Soc.* **163**, 77

Tayler R.J. 1980, *Mon. Not. Roy. Astron. Soc.* **191**, 151

Zahn, J.-P., Brun. A.S., Mathis, S. 2007, *Astron. Astrophys.* **474**, 145